Impact of the Casimir-Polder Potential and Johnson Noise on Bose-Einstein Condensate Stability Near Surfaces

Yu-ju Lin,* Igor Teper, Cheng Chin, and Vladan Vuletić

Department of Physics, Stanford University, Stanford, California 94305-4060, USA

We investigate the stability of magnetically trapped atomic Bose-Einstein condensates and thermal clouds near the transition temperature at small distances $0.5 \ \mu m \leq d \leq 10 \ \mu m$ from a microfabricated silicon chip. For a 2 μm thick copper film, the trap lifetime is limited by Johnson noise induced currents and falls below 1 s at a distance of 4 μm. A dielectric surface does not adversely affect the sample until the attractive Casimir-Polder potential significantly reduces the trap depth.

Bose-Einstein condensates in magnetic traps [1–5] and waveguides [3,6], and thermal atoms in waveguides [7] produced by microfabricated structures (microtraps), hold great promise for new quantum devices for atomic matter waves, such as Fabry-Pérot resonators [8], interferometers [9], or Josephson junctions [10]. Full quantum control over the motion of an ultracold atom of mass m and energy E requires potentials that vary abruptly on a length scale $\lambda \sim h/(mE)^{1/2}$, typically 1 μm. Such potentials can be created at small distances $d \leq \lambda$ from miniaturized field sources.

However, the proximity of a room-temperature surface can perturb the ultracold gas, and microtrap experiments have revealed condensate fragmentation [3,4,11], heating [1,11], and reduced trap lifetime [11]. The fragmentation has been traced to spatial variations of the longitudinal magnetic field near a conductor carrying current [12], while heating and loss have been eliminated for distances $d \gtrsim 70 \ \mu m$ by careful electronic design and shielding [4]. However, Jones *et al.* [13] and Harber *et al.* [14] have recently reported a fundamental limit due to spin flips induced by thermally excited currents in a mesoscopic conductor, in very good agreement with theoretical predictions [15] over the measurement regions $25 \ \mu m \leq d \leq 100 \ \mu m$ and $3 \ \mu m \leq d \leq 1 \ mm$, respectively.

In this Letter, we explore fundamental limitations on condensate stability at small distances down to $d = 0.5 \ \mu m$ from dielectric and metal surfaces. For a 2 μm thick copper film carrying no current, we observe a distance-dependent lifetime $\tau(d)$ that is quantitatively explained by thermal magnetic field fluctuations arising from Johnson noise induced currents [15,16]. For the dielectric, we observe a reduction in trap lifetime only when the vicinity of the surface limits the trap depth. A one-dimensional (1D) evaporation model can explain the measured trap loss, but only when the attractive Casimir-Polder force [17] between atoms and surface is included. Our results suggest that the local manipulation of condensates will be possible using thin conductors, which have low magnetic field noise, on dielectric surfaces.

The atom-surface interactions are studied using ultracold atoms confined in a Ioffe-Pritchard trap generated by currents flowing in microfabricated conductors on a silicon chip (see Fig. 1). The chip was produced by first coating a 300 μm thick silicon substrate with a 1 μm thick, electrically insulating Si_3N_4 diffusion barrier using plasma-enhanced chemical vapor deposition. Subsequently, a 20 nm thick Ti adhesion layer, a 2.15(20) μm thick Cu conducting layer, a 40 nm thick Ti, a 50 nm thick Pd, and a 100 nm thick Au layer were deposited by electron beam evaporation. Finally, the wires were defined by photolithography and wet etching.

The radial (xz) confinement of the Ioffe trap formed above the chip is provided by a 2D quadrupole field, generated by two copper wires Q along the y direction carrying antiparallel currents, in superposition with a bias field along z. The centers of the 2 μm thick and 20 μm wide Q wires are separated by 100 μm. The axial (y) confinement is created by a current-carrying gold ribbon P along x in combination with an external field gradient along y. The 25 μm thick, 150 μm wide ribbon 155 μm above the chip was wire bonded to the surface.

The condensate production starts with a standard magneto-optical trap (MOT), into which typically 10^7
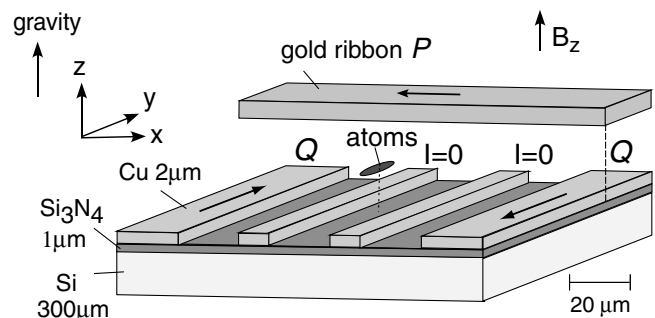

FIG. 1. Microfabricated chip. (Only the x direction is to scale.) The outer Cu wires (Q) generate a 2D quadrupole field in the xz plane. The ribbon (P) in combination with an external field gradient creates the confinement along y.

[87]Rb atoms are collected within 8 s from a Rb dispenser beam [2]. We then move the MOT cloud from the original distance $d = 17$ mm to within $d = 6$ mm of the chip surface, and compress it for 20 ms. After the MOT light has been extinguished, the atoms are optically pumped in 400 μs into the $F = 2$, $m = 2$ ground state, and loaded into a large quadrupole trap with x, y, z gradients of 33, 8, and 25 G/cm, respectively. Next, by increasing a bias field B_z generated by a small coil located 2 mm below the chip, the atoms are compressed in 300 ms into a Ioffe microtrap, where the conversion from quadrupole to Ioffe trap geometry follows Ref. [18]. The trap is located at $d = 50$ μm from the surface and 430 μm away from the P ribbon along y for currents of 0.6 A in both the Q wires and the P ribbon. For a field at trap bottom of $B_0 = 1.5$ G, the radial and axial vibration frequencies are $\omega_{rad}/2\pi = 5.1$ kHz and $\omega_{ax}/2\pi = 70$ Hz, respectively. We typically load 3×10^6 atoms at an initial temperature of 300 μK, peak density of 1.7×10^{12} cm^{-3}, and peak collision rate of 140 s^{-1}. Three seconds of forced evaporation cool the sample to below the transition temperature $T_c = 0.8$ μK. When the thermal component is no longer discernible in a time-of-flight image, the condensate contains 10^3 atoms at a peak density of $n_p = 8 \times 10^{14}$ cm^{-3}. To measure surface-induced loss, we transport the condensate or a cloud near T_c adiabatically in 40 ms to a defined position near the surface, hold it there for a variable time, and image the cloud after moving it back to $d = 100$ μm. The noise-equivalent-optical density of 1% in the absorption imaging corresponds to a small atom number noise $\delta N = 50$ for a condensate. The procedure is repeated for each parameter value.

In order to compare an observed influence of the surface to theoretical models, the accurate calibration of the trap position (x,z) in the xz plane is crucial. While optical imaging fails close to the chip, the calibration is facilitated by the symmetry of the photolithographically defined Q wires (see Fig. 1). The trap is located where a homogeneous external bias field, with x and z components (B_x, B_z), cancels the field from the Q wires. Once the bias field value (B_x^0, B_z^0) that places the trap at the symmetry center $(x = 0, z = 0)$ of the Q wires is known precisely, the atoms can be accurately positioned at arbitrary (x,z) by applying an additional field $(\Delta B_x, \Delta B_z) = (B_x - B_x^0, B_z - B_z^0)$ to compensate the spatially varying field from the Q wires. Figure 2(a) shows how the relative field $(\Delta B_x, \Delta B_z)$ maps to trap position (x,z). We also take into account a slight map distortion due to all other coils in the setup, which displaces the Ioffe trap by 0.50(5) μm away from the chip compared to the map defined by the Q wires alone.

To precisely measure the symmetry-center bias field (B_x^0, B_z^0) that depends on unknown stray fields, we make use of the reflection symmetry of the Q wire configuration. We exploit the fact that a mirror image trap, located at $(-x, -z)$, coexists with the trap at (x,z) [see Fig. 2(a)]. As the trap and the image trap are brought close, the
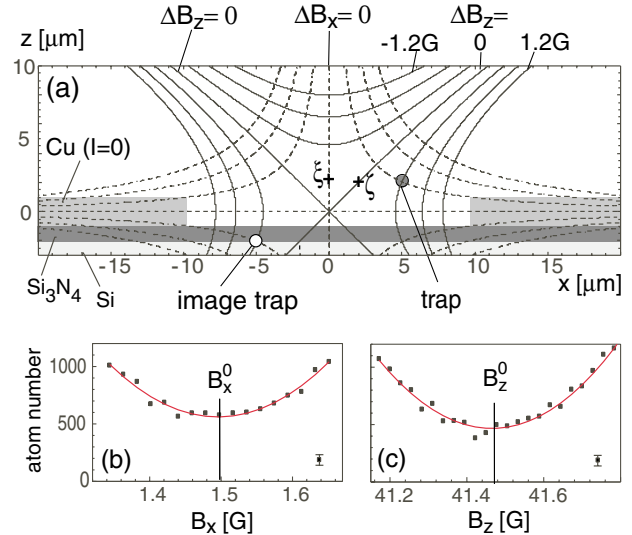

FIG. 2 (color online). (a) Map of relative field $(\Delta B_x, \Delta B_z)$ to trap position in the xz plane. Dashed (solid) lines are contours of ΔB_x (ΔB_z), plotted with 0.4 G spacing. (b),(c) Measured atom loss versus B_x (B_z) near point ξ (ζ), marked by a cross.

atoms can overcome the barrier between the traps, and will be lost if the image trap is inside the surface. Along a ΔB_z contour, the loss is symmetric about the point $\Delta B_x = 0$ [e.g., point ξ in Fig. 2(a)], where the minimum barrier leads to maximum loss. From the measured atom number versus ΔB_x along the $\Delta B_z = -120$ mG contour, we determine B_x^0 with a precision of $\delta B_x^0 = 4$ mG [Fig. 2(b)]. Similarly, B_z^0 is determined within $\delta B_z^0 = 10$ mG [Fig. 2(c)] by a measurement along the $\Delta B_x = 110$ mG contour near point ζ in Fig. 2(a). In the spatial region of interest, the uncertainties $(\delta B_x^0, \delta B_z^0)$ correspond to a trap z position error of 20 nm, small compared to a condensate size of 300 nm in the xz plane.

To verify that we can position the trap accurately relative to microscopic structures on the surface, we first measure a line of constant lifetime $\tau = 22$ ms near a Cu film carrying no current, shown as curve C in Fig. 3. This surface microscopy yields a contour that displays the expected symmetry about the metal, which confirms the
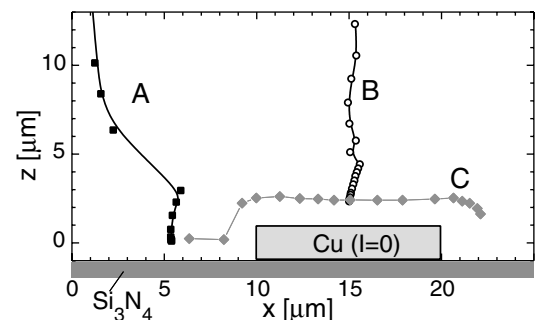

FIG. 3. Paths chosen for trap lifetime measurements above a dielectric surface (A) and above a copper film (B). Line C is the measured contour line of 22 ms lifetime near the metal.

skewed field-to-position mapping in Fig. 2(a). Figure 3 also shows the trajectories we then use to measure the lifetime above the Si_3N_4 dielectric (A) and the copper film (B). Path A is selected to avoid coupling to the image trap in the center region.

Figure 4 shows the lifetime τ as a function of distance d from the respective surface, measured at $T = 1\ \mu K$ ($T/T_c = 1.3$) for an offset field $B_0 = 0.57$ G. The lifetime above the dielectric is constant for $d \geq 2.5\ \mu m$, while above the metal τ is shorter and distance dependent. Since even a conductor carrying no macroscopic current generates magnetic field fluctuations associated with thermal current noise [16], it can induce trap decay by driving transitions from trapped to untrapped atomic sublevels [15]. In the limit that the metal film thickness [here $t = 2.15(20)\ \mu m$] is much smaller than the skin depth δ at the transition frequency ($\delta = 103\ \mu m$ for $B_0 = 0.57$ G), the current noise is the Johnson noise in the conductor, and is frequency independent. (The measurements in Refs. [13,14] were performed in the opposite limit, $t \gg \delta$, of a bulk metal.) Then for a metal film of width $w \gg t$, and resistivity ρ at temperature T, the spin flip rate $|F, m\rangle \rightarrow |F, m - 1\rangle$ is given by $\Gamma_{Fm} = C_{Fm}^2 C_0 [d(1 + d/t)(1 + 2d/w)]^{-1}$. This formula interpolates the loss rates predicted by Henkel $et\ al.$ [15] in the limits $d \ll w$ and $d \gg w$. We derive Γ_{Fm} at $d \gg w$ from Ref. [15] assuming only thermal currents along the wire contribute substantially. Here $C_{Fm}^2 = |\langle F, m - 1|S_-|F, m\rangle|^2$, S_- is the electron spin lowering operator, $C_0 = 88\ s^{-1}\ \mu m \times (T/300\ K)(\rho_{Cu}/\rho)$, $\rho_{Cu} = 1.7 \times 10^{-8}\ \Omega$ m, $T = 400$ K from the measured ρ/ρ_{Cu}, and $w = 10\ \mu m$. We assume the atoms are lost in a cascade process, $|2, 2\rangle \rightarrow |2, 1\rangle \rightarrow |2, 0\rangle$, replace C_{Fm}^2 by $(C_{22}^{-2} + C_{21}^{-2})^{-1} = (4 + \frac{8}{3})^{-1}$, and add the distance independent one-body loss rate $\gamma_1 = 0.4\ s^{-1}$ observed at $d \geq 10\ \mu m$. The result (solid line) agrees well with the observed lifetime above the thin copper film. For comparison, the fundamental limit due to the thermal field noise only ($\gamma_1 = 0$) is plotted as a dotted line. Except for the point closest to the metal surface, τ is independent of sample temperature, indicating that the loss process is not evaporation at finite trap depth. Further, the lifetime $\tau(d)$ measured for $B_0 = 1.5$ G, i.e., at a 3 times larger transition frequency, is compatible with the white field noise within 40%.

Above the dielectric, the constant lifetime $\tau = 3.5$ s observed for $d > 2.5\ \mu m$ is independent of cloud temperature for $1\ \mu K \leq T \leq 3\ \mu K$, and the latter remains constant within our resolution of $0.25\ \mu K/s$. In the short-distance region of decreasing lifetime, however, τ is longer for a colder cloud, which is consistent with surface-induced 1D evaporation [14,19]. To test this explanation, we measure the remaining atom fraction χ after 15 ms versus d for a condensate, and for thermal clouds at 2.1 and 4.6 μK (Fig. 5). A thermal cloud exhibits loss at a larger distance than a condensate, and the latter vanishes at a finite distance $d = 1\ \mu m$.
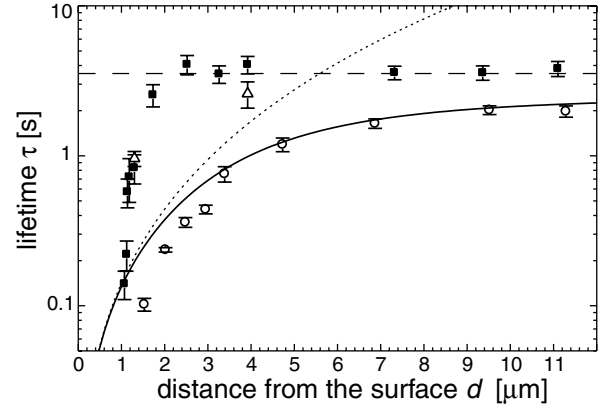
FIG. 4.   Trap lifetime as a function of distance from a dielectric (solid squares) and metal (open circles) surface, for $T = 1\ \mu K$ and $B_0 = 0.57$ G. The dotted line is the calculated lifetime above the metal due to thermal B fields only, the solid line includes the one-body lifetime. The open triangles are measurements for a pure condensate above the dielectric.

In the absence of atom-surface interactions, the trap depth would be given by the value of the trapping potential at the surface. However, as shown in the inset of Fig. 5, the attractive Casimir-Polder potential [17], $V_{CP} = -C_4/d^4$, lowers the trap depth, and the trap disappears at finite d. To quantify this effect, we model the process as a sudden loss of the Boltzmann tail as the atoms are brought near the surface, in conjunction with 1D evaporation for $t_0 = 15$ ms in a trap with $\omega_{rad}/2\pi = 3.6$ kHz. The remaining fraction after the sudden loss is given by $F = 1 - e^{-\eta}$, where $\eta = U_0/(kT)$ is the ratio of the Casimir-force limited trap depth $U_0(d)$ and thermal energy kT. We account for atom tunneling through the barrier as a small reduction in the effective trap depth. The loss rate for 1D evaporation is $\Gamma = f(\eta)e^{-\eta}/\tau_{el}$, which using $f(\eta) = 2^{-5/2}(1 - \eta^{-1} + \frac{3}{2}\eta^{-2})$ is accurate to 5% for $\eta \geq 4$ [20]. Given elastic collision times $\tau_{el} = 0.2$, 0.9, and 1.5 ms for the condensate, the 2.1 and the 4.6 μK clouds, respectively, we plot in Fig. 5 the remaining fraction $\chi_{CP} = Fe^{-\Gamma t_0}$. For the condensate, we assume that the loss is due to collisions between a residual thermal cloud at $T_c/2$ and the condensate. For the Casimir potential, we use the coefficient $C_4 = \psi(\varepsilon)3\hbar c\alpha/(32\pi^2\epsilon_0)$, where $\alpha = 5.25 \times 10^{-39}$ F m^2 is the Rb polarizability, and $\psi(\varepsilon) = 0.46(5)$ is a numerical factor from Ref. [21] for the Si_3N_4 dielectric constant of $\varepsilon = 4.0(8)$. For comparison, we also plot the calculated fraction in the absence of any surface potential ($C_4 = 0$).

Figure 5 can be interpreted as a measurement of the Casimir-Polder coefficient C_4 that is, however, limited by the uncertainty of the distance calibration. The dominant contribution of ± 100 nm arises from a ± 200 nm uncertainty of the conductor thickness t (see Fig. 2). In addition, an estimated 10% field calibration uncertainty for ΔB_x contributes a 10% scaling error about the distance $d_0 = 1.6\ \mu m$. Furthermore, our setup with a 1 $\mu m\ Si_3N_4$ layer on Si is a dielectric waveguide. The corresponding
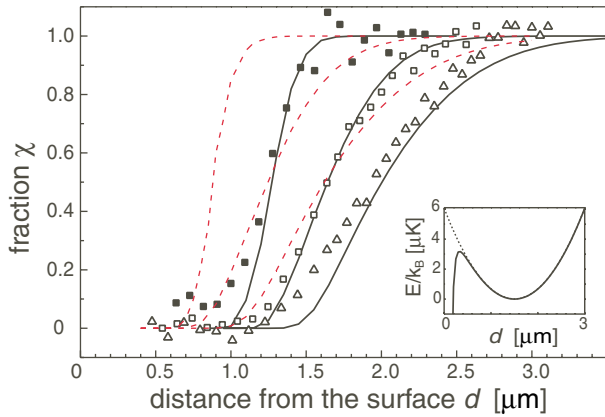
FIG. 5 (color online). Remaining atom fraction χ in a trap at distance d from the dielectric surface for a condensate (solid squares), and for thermal clouds at 2.1 μK (open squares) and 4.6 μK (triangles). The solid (dashed) lines are calculated with (without) Casimir-Polder potential for the condensate, 2.1 μK, 4.6 μK clouds (left to right). The inset shows the trapping potentials for $C_4 = 8.2 \times 10^{-56}$ J m^4 (solid line) and $C_4 = 0$ (dotted line).

correction to C_4 compared to a Si$_3$N$_4$ half-space is estimated to be less than 20% [22]. Uncertainties in temperature and trap vibration frequency of 10% also affect $\chi_{CP}(d)$. When we take these error sources into account, our measurements in combination with the 1D evaporation model imply a 66% confidence range for C_4 between 1.2×10^{-56} and 41×10^{-56} J m^4, which includes the nominal value $C_4 = 8.2 \times 10^{-56}$ J m^4. The good agreement between our data and the predicted C_4 without any adjustment of parameters suggests that the Casimir potential limits the trap depth, and consequently lifetime, at small distances $d \lesssim 2$ μm from the dielectric surface. The discrepancy at small fraction χ is probably due to our simple 1D evaporation model which breaks down for $\eta \lesssim 1$, and also ignores evaporation-induced temperature changes. Our data exclude $C_4 = 0$, even if we allow for the largest possible systematic error.

In conclusion, we have characterized the stability of magnetically trapped ultracold atoms at μm distances from a copper film and a dielectric surface. The condensate is stable over the dielectric, and the spectral density of the thermal magnetic field near a metal film scales with metal thickness. Therefore it will be possible to bring a stable ultracold cloud sufficiently close to the surface for the trapping potential to be locally manipulated.

Note added.—The Casimir potential cannot explain the anomalously short lifetime at the smallest distance $d = 1.5$ μm above the metal (see Fig. 4 and the "surface microscopy" curve C in Fig. 3). One possible explanation is patch potentials from Rb atoms adsorbed on the metal, as recently reported by McGuirk *et al.* [23].

*Present Address: MIT-Harvard Center for Ultracold Atoms, MIT, Cambridge, MA 02139, USA.

[1] W. Hänsel, P. Hommelhoff, T.W. Hänsch, and J. Reichel, Nature (London) **413**, 498 (2001).

[2] H. Ott, J. Fortágh, G. Schlotterbeck, A. Grossmann, and C. Zimmermann, Phys. Rev. Lett. **87**, 230401 (2001).

[3] A. E. Leanhardt, A. P. Chikkatur, D. Kielpinski, Y. Shin, T. L. Gustavson, W. Ketterle, and D. E. Pritchard, Phys. Rev. Lett. **89**, 040401 (2002).

[4] A. E. Leanhardt, Y. Shin, A. P. Chikkatur, D. Kielpinski, W. Ketterle, and D. E. Pritchard, Phys. Rev. Lett. **90**, 100404 (2003).

[5] S. Schneider, A. Kasper, C. vom Hagen, M. Bartenstein, B. Engeser, T. Schumm, I. Bar-Joseph, R. Folman, L. Feenstra, and J. Schmiedmayer, Phys. Rev. A **67**, 023612 (2003).

[6] J. Fortágh, H. Ott, S. Kraft, A. Günther, and C. Zimmermann, Appl. Phys. B **76**, 157 (2003).

[7] D. Müller, D. Z. Anderson, R. J. Grow, P. D. D. Schwindt, and E. A. Cornell, Phys. Rev. Lett. **83**, 5194 (1999); N. H. Dekker, C. S. Lee, V. Lorent, J. H. Thywissen, S. P. Smith, M. Drndić, R. M. Westervelt, and M. Prentiss, *ibid.* **84**, 1124 (2000).

[8] M. Wilkens, E. Goldstein, B. Taylor, and P. Meystre, Phys. Rev. A **47**, 2366 (1993).

[9] Y. Shin, M. Saba, T. A. Pasquini, W. Ketterle, D. E. Pritchard, and A. E. Leanhardt, cond-mat/0306305.

[10] B. Anderson and M. Kasevich, Science **282**, 1686 (1998).

[11] J. Fortágh, H. Ott, S. Kraft, A. Günther, and C. Zimmermann, Phys. Rev. A **66**, 041604(R) (2002).

[12] S. Kraft, A. Günther, D. Wharam, C. Zimmermann, and J. Fortágh, J. Phys. B **35**, 469 (2002).

[13] M. P. A. Jones, C. J. Vale, D. Sahagun, B V. Hall, and E A. Hinds, Phys. Rev. Lett. **91**, 080401 (2003).

[14] D. M. Harber, J. M. McGuirk, J. M. Obrecht, and E. A. Cornell, J. Low Temp. Phys. **133**, 229 (2003).

[15] C. Henkel, S. Pötting, and M. Wilkens, Appl. Phys. B **69**, 379 (1999); C. Henkel and S. Pötting, Appl. Phys. B 72, 73 (2001).

[16] T. Varpula and T. Poutanen, J. Appl. Phys. **55**, 4015 (1984).

[17] H. B. G. Casimir and D. Polder, Phys. Rev. **73**, 360 (1948); C. I. Sukenik, M. G. Boshier, D. Cho, V. Sandoghdar, and E. A. Hinds, Phys. Rev. Lett. **70**, 560 (1993).

[18] J. Fortágh, A. Grossmann, C. Zimmermann, and T.W. Hänsch, Phys. Rev. Lett. **81**, 5310 (1998).

[19] J. Reichel, W. Hänsel, and T.W. Hänsch, Phys. Rev. Lett. **83**, 3398 (1999).

[20] W. Ketterle and N. J. Van Druten, Adv. At. Mol. Opt. Phys. **37**, 181 (1996); E. L. Surkov, J. T. M. Walraven, and G.V. Shlyapnikov, Phys. Rev. A **53**, 3403 (1996).

[21] Z.-C. Yan, A. Dalgarno, and J. F. Babb, Phys. Rev. A **55**, 2882 (1997).

[22] J.-Y. Courtois, J.-M. Courty, and J. C. Mertz, Phys. Rev. A **53**, 1862 (1996).

[23] J. M. McGuirk, D. M. Harber, J. M. Obrecht, and E. A. Cornell (to be published).